A novel fabrication technique to minimize PDMS-microchannels deformation under high-pressure operation.

ARTICLE *in* ELECTROPHORESIS · DECEMBER 2013

Impact Factor: 3.16 · DOI: 10.1002/elps.201300340 · Source: PubMed

4 AUTHORS:

Hojjat Madadi
École Supérieure de Physique et de Chimie …
22 PUBLICATIONS **8** CITATIONS
SEE PROFILE

Mahdi Mohammadi
Dublin City University
18 PUBLICATIONS **1** CITATION
SEE PROFILE

Jasmina Casals-Terré
Polytechnic University of Catalonia
47 PUBLICATIONS **111** CITATIONS
SEE PROFILE

Robert Castilla
Polytechnic University of Catalonia
34 PUBLICATIONS **94** CITATIONS
SEE PROFILE

Hojjat Madadi
Mahdi Mohammadi
Jasmina Casals-Terré
Roberto Castilla López

Technical University of Catalonia, Mechanical Engineering Department, Terrassa, Spain

Received May 11, 2013
Revised August 21, 2013
Accepted September 2, 2013

Research Article

A novel fabrication technique to minimize poly(dimethylsiloxane)-microchannels deformation under high-pressure operation

PDMS is one of the most common materials used for the flow delivery in the microfluidics chips, since it is clear, inert, nontoxic, and nonflammable. Its inexpensiveness, straightforward fabrication, and biological compatibility have made it a favorite material in the exploratory stages of the bio-microfluidic devices. If small footprint assays want to be performed while keeping the throughput, high pressure-rated channels should be used, but PDMS flexibility causes an important issue since it can generate a large variation of microchannel geometry. In this work, a novel fabrication technique based on the prevention of PDMS deformation is developed. A photo-sensible thiolene resin (Norland Optical Adhesive 63, NOA 63) is used to create a rigid coating layer over the stiff PDMS micropillar array, which significantly reduces the pressure-induced shape changes. This method uses the exact same soft lithography manufacturing equipment. The verification of the presented technique was investigated experimentally and numerically and the manufactured samples showed a deformation 70% lower than PDMS conventional samples.

Keywords:
Microchannel-integrated micropillars / Microfabrication technique / PDMS deformation
DOI 10.1002/elps.201300340

Additional supporting information may be found in the online version of this article at the publisher's web-site

1 Introduction

Soft lithography is a low-cost and consolidated method that plays a major role in the microfluidics fabrication. Outstanding PDMS characteristics, such as compatibility with organic and inorganic systems, make it a valuable tool for performing fundamental studies of cell biology and tissue engineering in the exploratory stages of research, and if small footprint assays want to be performed while keeping the throughput high pressure-rated channels should be used [1, 2]. In spite of many advantages of PDMS and its broad use in biological laboratories, it has some drawbacks like hydrophobicity and low elastic modulus, which cause significant issues in high-pressure operation [3]. In terms of PDMS hydrophobicity, many works have been done on the surface modification of PDMS [4, 5] while few studies have discussed the importance of PDMS channel deformation in microfluidics. The low elastic modulus of PDMS offers some advantages like easy replica molding without damage to features. However, this property has also been shown to generate a large variation of microchannel geometry and have broad impacts in microfluic device performance [6]. There are a number of alternative materials to PDMS that overcome the problem of pressure-induced deformation such as polycarbonate (PC) [7], cyclic olefin copolymer (COC) [8], and PMMA [9], but they require high initial cost of the molding equipment and expertise since they use hot embossing, laser ablation, or injection molding [10]. Besides, the bonding strength of these materials is another issue that needs further advances to meet various microfluidic applications without sacrificing its native material properties after bonding [11], in this regard Roy et al. [12] improved the thermoforming method with simplified equipment. On the other hand, materials that can be casted as PDMS but with higher rigidity such as thermoset polyester (TPE), polyurethane methacrylate (PUMA), or Norland Optical Adhesive 81 (NOA 81) have been studied [13–15]. The fabrication process for these materials is slightly different to the soft lithography. The substrates first are semicured using UV light and unmolded, later the curing is finished once the cover is fixed on the top of the microchannel. The

Correspondence: Dr. Jasmina Casals-Terré, Microsystem Laboratory, Department of Mechanical Engineering, Technical University of Catalonia, Terrassa 08222, Spain
E-mail: Jasmina.casals@upc.edu

Abbreviations: **h-PDMS**, hard PDMS; **MIMP**, microchannel-integrated micropillars; **NOA**, Norland Optical Adhesive; **TPE**, thermoset polyester

Colour Online: See the article online to view Figs. 1–10 in colour.

step of unmolding a semicure material is critical since for long-length channel it can cause deformation. Sollier et al. [16] suggested TPE (1.2 GPa) as the best alternative to PDMS particularly for high-pressure operation. A main drawback of TPE is related to TPE fabrication process, which needs precisely weighing and mixing several components under a fume hood because of the toxic fumes from the resin, besides considering the cost of TPE that is more than four times as compared to PDMS. Additionally, by considering the results of Sollier et al.'s work, the biocompatibility of TPE is another issue while its suitability for cell culture is largely unknown [16].

The relevance and validity of PDMS in microfluidics design and manufacturing have driven the researchers to carefully analyze and monitor the impact of its low Young Modulus. For instance to measure the PDMS deformation, first Hosokawa et al. presented a method for local pressure monitoring in microfluidic devices using a deformable diffraction grating but they did not provide the magnitude of channel deformation with respect to the imposed flow rate [17]. In another work, Holden and his colleagues experimentally determined the bulk PDMS deformation under high pressure by utilizing the variation in fluorescence intensity with channel bulging [18]. They measured the change of PDMS microchannel cross-section as a function of flow rate. Later, Gervais et al. found that PDMS deformation is a very important performance issue in low aspect ratio channels [3]. To quantify the deformation of microchannels under pressure-driven flows, Hardy and his colleagues presented a method that used fluorescence microscopy [6]. They found that the pressure drop decreased up to 35% less than the pressure drop in a rigid-wall microchannel and they figured out that as wall thickness decreased, this effect was magnified. Recently, Sollier et al. employed fluorescence microscopy to measure PDMS channel deformation. They found that the PDMS channel deformation is significant in both *X* and *Y* directions even at low flow rate, which leads to channel cross-sections higher and wider than expected [16].

Other works have focused on reducing the pressure-induced deformation; Inglis presented a method to sandwich the PDMS channel between two glass slides [19]. Although the deformation is reported to be three times less than for the standard PDMS channel, the glass-PDMS-glass assembly is restricted to some applications where simple outlet/inlet designs are required, since they have to be machined in glass, complicating the fabrication process.

Hard PDMS or h-PDMS is another alternative to standard PDMS, which was developed at IBM Zurich for nanoscale soft-lithography [20]. h-PDMS Young's modulus is 4.5 times higher than standard PDMS [21] but is very viscous and therefore, replicating h-PDMS complex geometries like microchannel-integrated micropillars (MIMP) from a master mold is an issue, which is mentioned by Inglis [19].

Another available option is to increase the hardness of standard PDMS by changing the amount of cross-linking agent from 10:1 ratio to 10:2. Armani et al. [22] reported that the elastic modulus of PDMS with the twice amount of cross-linker increased from 750 to 870 kPa, which solely is not enough to withstand high-pressure operation.

Hence, in this work to overcome the PDMS deformation under high-pressure operation, a novel technique is introduced that combines the use of stiff PDMS (10:2, the ratio between polymer base and cross-liking agent) and a thin coating layer of the UV curable thiolene resin as supporter (NOA 63) on the fabricated PDMS microchannel, see steps L and M in Fig. 1. The major advantages of this method are: simple and inexpensive fabrication, which does not need a complicated process. The verification of the presented technique was tested by considering MIMP as a complex geometry under high-pressure operation. This geometry is used in different regimes for bio-microfluidic device applications such as cell separation microdevices or microcapillary pumping devices. Several MIMP channels were fabricated showing a deformation up to 70% less than the same samples fabricated with standard PDMS.

This paper is structured as follows: The details of fabrication procedure are described in Section 2, the experimental analysis follows in Section 3, describing two different experiments to verify the proposed technique, some applications of the presented fabrication technique are enumerated in Section 4, and finally the conclusions are presented in Section 5.

2 Fabrication procedure

SU-8 is a negative tone photo-epoxy, which can be employed as a master mold in soft lithography. SU-8 (GM 1050, Gersteltec Sarl., Switzerland) was chosen since it can be used in thin films, between 3 and 8 μm. As the shallower channels are more sensitive to deformation and will show largely variations in their cross-sectional area [3] 6 μm-depth channels are used.

The prepared designed mask was printed in a high-resolution film. Microscopy glass slides of 75 × 25 mm were utilized as substrates, which were first cleaned by Piranha cleaning process (3:1 of H_2SO_4/H_2O_2; see step A in Fig. 1) and preheated on the hotplate at 200°C for 30 min to ensure that the glass slide dried completely.

After cooling the substrate, a 6 μm layer of the photoresist (SU-8) was spin coated at 1400 RPM during 40 s on the top of glass slide (see B in Fig. 1). The coated substrate was soft-baked at 120°C for 2 min and cooled down to the room temperature. The structures were patterned through the high-resolution printed photo mask by using 5.1 s UV exposure lamp (see step C in Fig. 1). The coated substrate was postexposure baked in two steps: 1 min at 65°C and 10 min at 95°C (see step D in Fig. 1), which leads to achieving full cross-linking. Then, the structure was cleared through the development process in PGMEA (propylene glycol methyl ether acetate) for 22 s and used as mold (see step E in Fig. 1). To make stiff PDMS micropillars integrated in the microchannel, Dow Corning Sylgard 184 silicone elastomer and curing agent were thoroughly mixed in the ratio 10:2 in weight. In order to ensure the easy peel off of the channels once cured,

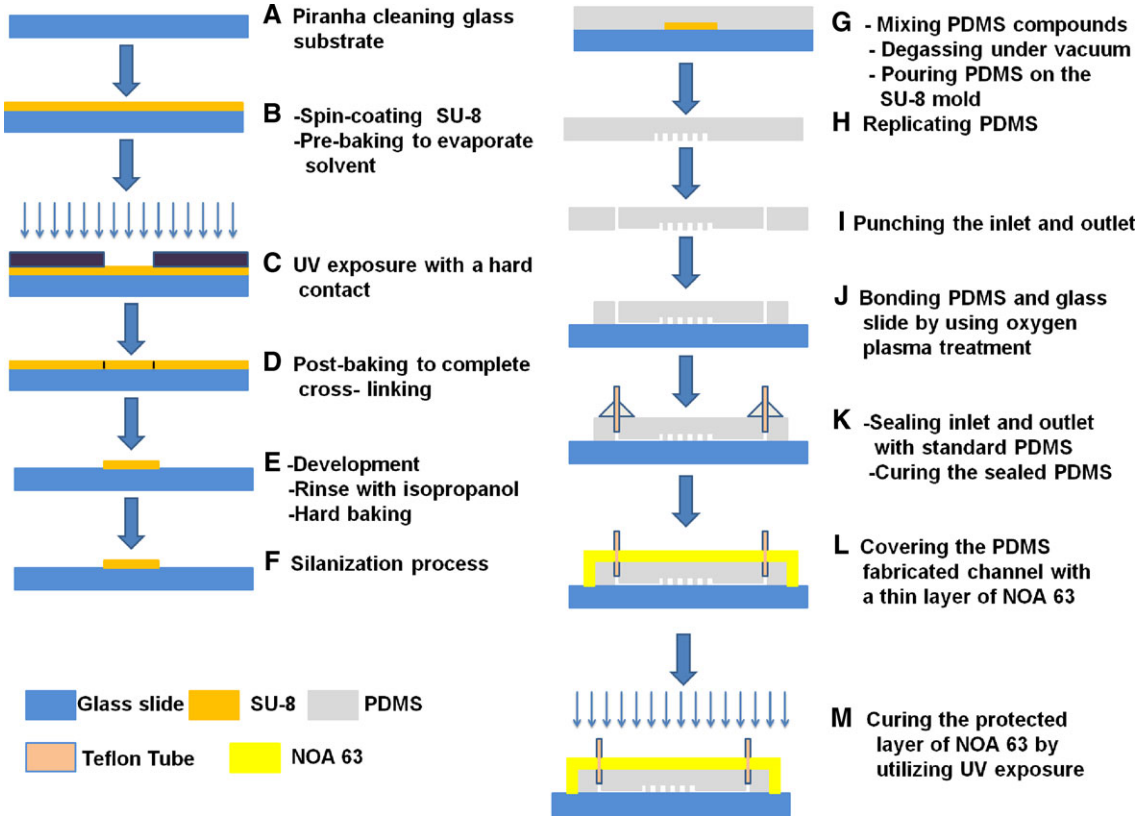

Figure 1. Fabrication steps of low deformation PDMS microchannels.

the mold was silanized (see step F in Fig. 1). The volume of the PDMS mixture was quantified to warranty 1 mm PDMS thickness. After the mixture was poured on the SU-8 master mold and then degassed in vacuum for 1 h, it was finally cured for 60 min at 85°C (see step G in Fig. 1). After curing, the PDMS MIMP channel was peeled off from the mold with ethanol (see step H in Fig. 1). In the next step, the inlet and outlet were punched (see I in Fig. 1).

Bonding the PDMS cast to a clean glass slide via an oxygen plasma treatment formed the enclosed microchannel (see step J in Fig. 1). Oxygen at 200 Torr was introduced in the oxygen plasma chamber (Gambetti) and the plasma was run for 30 s. The oxygen plasma parameters were chosen to achieve the maximum bond strength so that the channel could withstand up to 500 kPa [23]. The inlet and outlet of the microfluidic device were formed using two pieces of Teflon pipe, see Fig. 2 (see step K in Fig. 1).

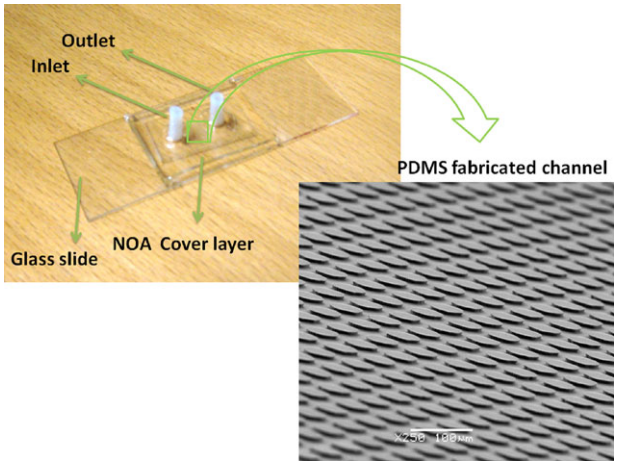

Figure 2. Optical image and SEM image of a fabricated MIMPs.

A thin layer of NOA 63 was used to coat and restrain the entire PDMS microchannel and the glass edges (see Fig. 1 step L). The NOA-coated microfluidic device was UV exposed for 6 s to complete NOA–glass bonding and constrained the PDMS microchannel between the glass and the NOA layer.

In this technique, the sealed glass slide to the channel is rigid, which imposes a zero-displacement boundary condition along the PDMS–glass interface, and the channel roof is constrained by a rigid coating layer of NOA 63 that leads to minimize the lateral displacement of channel walls and pillars.

3 Experimental validation

3.1 NOA-coated channels deformation compared to standard PDMS channels

In order to verify the presented technique, two MIMP designs were fabricated: one using standard PDMS (Fig. 1 steps A–J) and another using glass–PDMS–NOA (Fig. 1 steps A–M). The

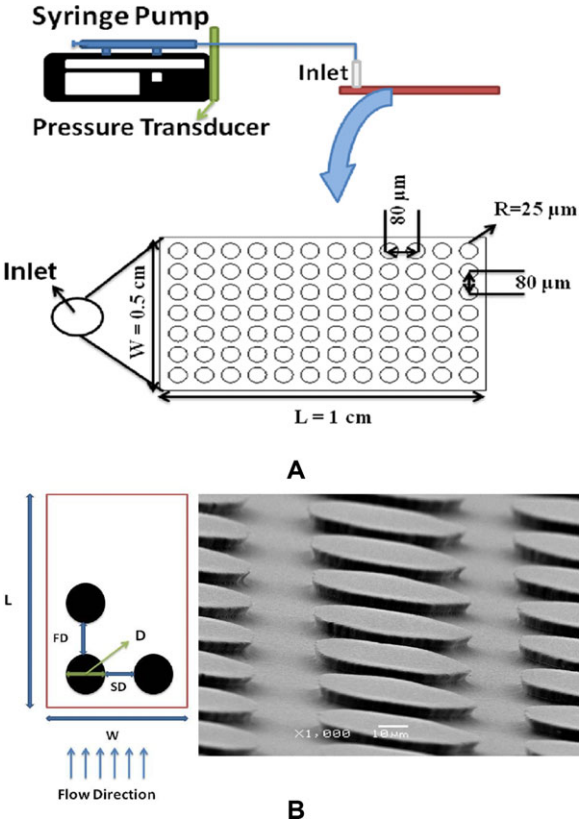

Figure 3. (A) Design of fabricated MIMPs and (B) schematics of the pillar arrangements and SEM picture of the fabricated PDMS pillars.

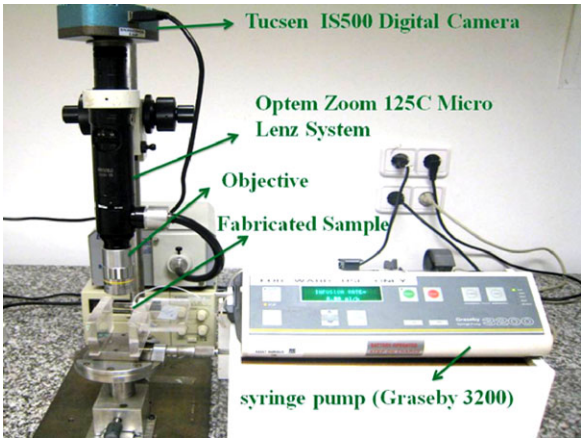

Figure 4. The experimental setup used to pressurize the fabricated samples and record its deformation.

design of the fabricated samples is shown in Fig. 3. During the punching step only one hole was created as inlet.

The fabricated samples were placed under various pressures while the channel outlet was kept sealed so there was no flow and the pressure was uniform all over the channel. Deionized water was used as testing fluid. The microchannel inlet was connected to the syringe pump (Graseby 3200, Smiths Medical, USA) while the outlet as mentioned earlier was sealed. Teflon tubing was employed to ensure leak proof connection between the pressure transducer and the microchannel inlet.

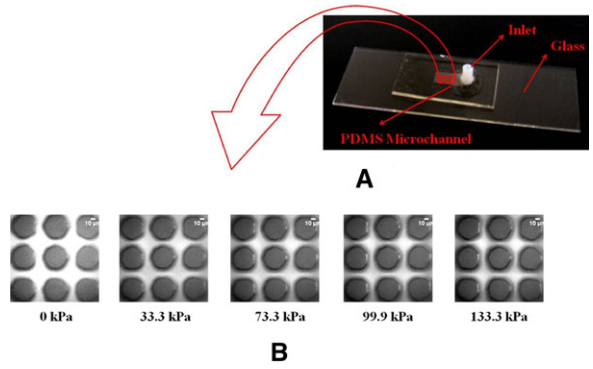

Figure 5. (A) Optical image of standard PDMS–glass fabricated sample and (B) micropillars before and under pressurization from 0 to 133.3 kPa.

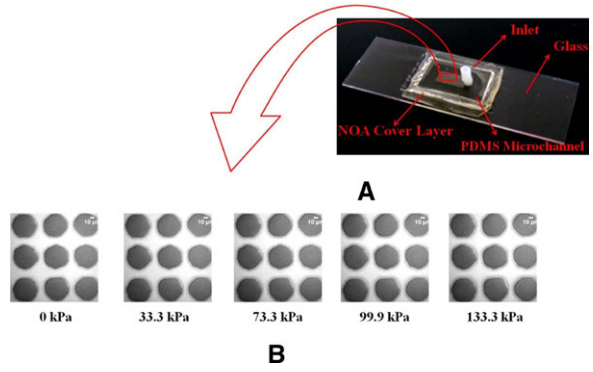

Figure 6. (A) Optical image of glass–PDMS—NOA 63 fabricated sample and (B) micropillars before and under pressurization from 0 to 133.3 kPa.

When the PDMS–glass channel was pressurized, the pillars that were attached to PDMS on one side and to the glass on the other deformed. This deformation was seen in the microscope as a blur ring around the pillars. In order to record images of the pillar deformation at various pressures and analyze this effect, a digital camera (Tucsen ISH500, 5.0 M pixel) was connected to a microinspection lens system Optem zoom 125C (with a broad 12.5:1 zoom range) and a 20× objective, see Fig. 4.

Figure 5 shows the evolution of this ring in the standard PDMS-fabricated samples when pressurized from 0 to 133 kPa. Generally, the PDMS pillars deformation depends on the local geometry and it leads to wider and deeper microfluidic channels than originally intended.

The same test was performed to glass–stiff PDMS–NOA fabricated samples pressurizing from 0 to 133 kPa. Figure 6 shows that the ring is almost negligible in the pillars fabricated using this modified microfabrication technique after applying 133.3 kPa pressure.

The distance between post rings was measured at all pressures and plotted in Fig. 7. As expected, the pillar deformation

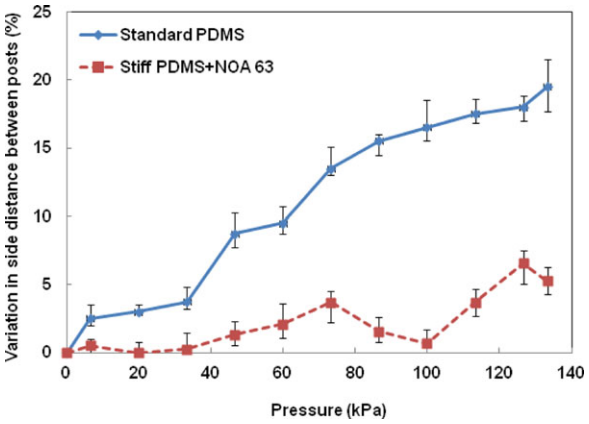

Figure 7. Comparison between change in side distance between posts at different pressures for (A) standard PDMS and (B) stiff PDMS with NOA coating layer.

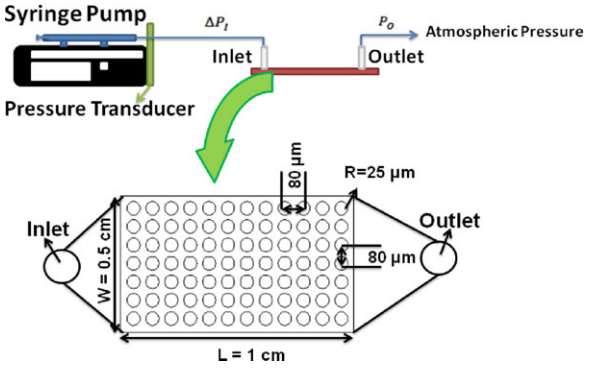

Figure 8. Schematic of the experimental setup for pressure drop measurements in the fabricated samples.

in the standard PDMS microchannel increased drastically when the pressure increased, but in glass–stiff PDMS–NOA samples this increment is significantly much less than in the standard samples at the same pressure. It can be highlighted that the side distance between post rings increased 19.5% after applying 133.3 kPa for the standard PDMS-fabricated sample, while this value decreased to 5.3% for the samples using the novel fabrication technique presented in this paper, which means that the channel deformation was reduced more than 70% using the presented technique.

3.2 Pressure drop comparison between NOA-coated channels and a numerical simulation model assuming rigid wall boundary conditions

To prove the efficiency of the presented fabrication technique, another independent experiment was accomplished. In this experiment, the effect of the channel deformation reduction is monitored using the relationship between the total pressure drop over a channel section and the resulting flow rate, which is then compared to a rigid microchannel case. When the MIMP is considered as the microchannel

Table 1. Average dimensions of the NOA-coated samples (µm)

Sample	D	SD	FD	H	W	L
Circle	52	28	32	6	4960	10 000

Note: D, Diameter; SD, side distance; FD, forward distance; H, height; W, width; L, length.

filled with porous media, based on the Darcy's law for the steady-state low Reynolds number flow, the pressure drop varies linearly with the imposed flow rate [24]. To demonstrate the reduced effects of microchannel deformation on flow behavior when the presented fabrication technique is used, the pressure drop was measured experimentally through MIMP while the outlet was kept open to the atmosphere (see Fig. 8) and compared to the obtained pressure drop in a numerical simulation model of the same geometry but assuming rigid wall boundary conditions. The average dimensions of the manufactured devices have been listed in Table 1.

A laminar flow was generated using a syringe pump and a pressure transducer was used to measure the in-line pressure, see Fig. 8. The total measured pressure drop is a summation of different effects:

$$\Delta P_{\text{total}} = \Delta P_{\text{I}} + \Delta P_{\text{en}} + \Delta P_{\text{FD}} + \Delta P_{\text{minor}} + \Delta P_{\text{ev}}, \quad (1)$$

where ΔP_{I} is the pressure drop in the connecting, tube which was measured directly at each flow rate, ΔP_{en} is the pressure drop in the inlet region, ΔP_{FD} is the pressure drop in the fully developed region of the microchannel, ΔP_{minor} is the pressure drop due to the bends in the microchannel inlet, and ΔP_{ev} is the pressure drop due to the electroviscous effect [25].

Akbari et al. [25] showed that ΔP_{minor} and ΔP_{ev} are less than 1% of the pressure drop in the fully developed region, ΔP_{FD}, and therefore they could be neglected. On this basis, the measured pressure drop in the microchannel was related to the pressure drop in the fully developed region of the microchannel once ΔP_{I} had been determined.

The experimental values of pressure drop are plotted in Fig. 9, which show an almost linear relationship with volumetric flow rate.

These results were also compared to the obtained numerical values of pressure drop and resistance flow versus the volumetric flow rate of the flow through a microchannel with integrated rigid micropillars. This numerical analysis was performed using Ansys Fluent 12.0.1 software, which is based on finite volume method (ANSYS Academic Research, Fluent 12.0 User's Guide, ANSYS, Inc. 2009.).

The produced numerical grid and the obtained velocity contour of the considered model by Ansys Fluent are shown in Fig. 10. More details about numerical modeling are presented in the Supporting Information.

According to the numerical results of the pressure drop plotted in Fig. 9, the difference between the measured data and the predicted values from numerical simulation is less than 10%. Hardy et al. [6] showed that the pressure drop through PDMS microchannel is up to 35% less than the pressure drop in the same sized channel with rigid walls.

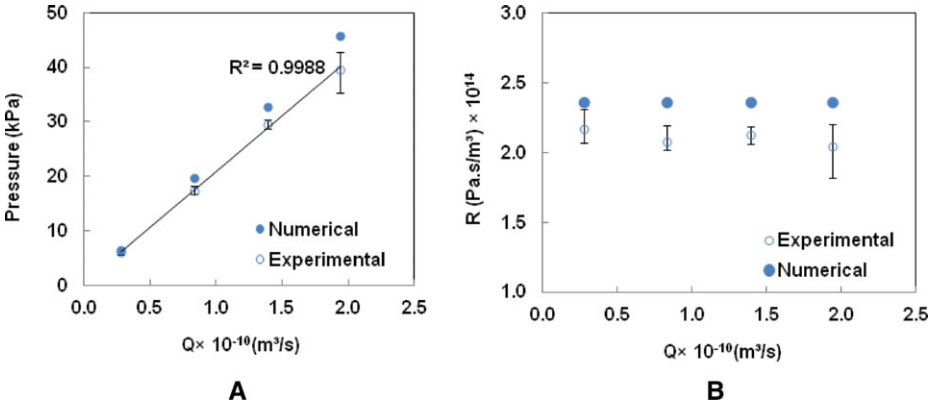

Figure 9. Numerical (rigid walls) and experimental (with NOA-coated layer) (A) pressure drop and (B) resistance flow in integrated micropillar microchannels at different flow rates.

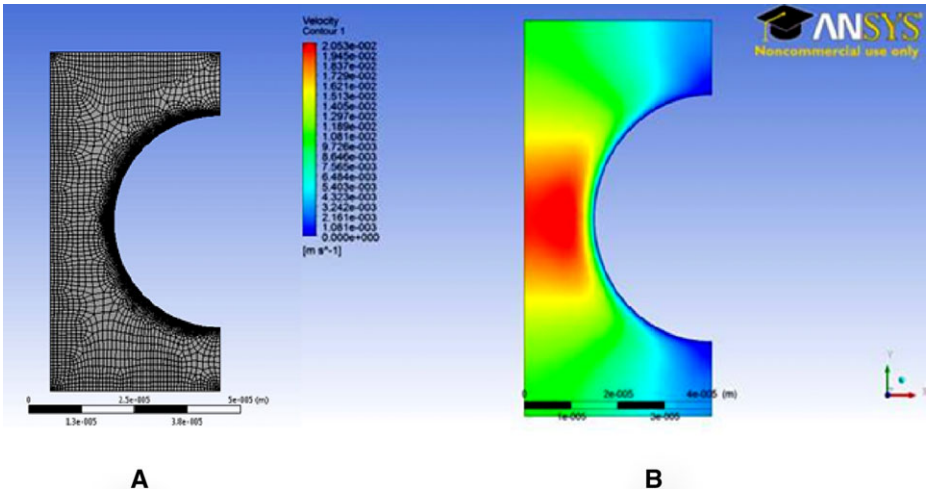

Figure 10. (A) The produced numerical grid and (B) the velocity contour of considered unit cell.

Since numerical results assume rigid walls, this small mismatch (<10%) corroborates that the reduction of PDMS deformation when using NOA-coated layer is more than 70% in comparison to the standard PDMS fabrication method. Although this new fabrication technique tends to minimize the deformation, there is still some deformation that cannot be completely eliminated and would justify the pressure drop difference.

4 Application

The deformation of a microfluidic channel significantly affects the effective pressure drop across it and the resulting flow profile, therefore the channel deformation minimization is valuable for any microfluidic application and precise knowledge of the flow profile, pressure, and channel geometry is needed. In order to compute the effective shear rate, the actual flow profile needs to be accurately determined in applications such as cellular and protein shear-flow assays [26–28]. Flow profile and channel height are also important parameters in the diffusion-limited mass transfer applications [29]. The increase in the channel's effective height causes enhancement in Taylor dispersion and affects the performance of a system to resolve intrinsic surface kinetics like surface plasmon resonance (SPR) in lab-on-a-chip sensor applications [30]. Recently, Di Carlo and coworkers showed that PDMS deformability affects inertial focusing and they confirmed that particle distribution, which is dependent on cross-section geometry, is also a function of material deformability [16], since it strongly relies on precisely determined gap distances between posts.

Therefore if a deterministic lateral displacement phenomenon needs to be used for separating particles in small footprint assays while keeping the throughput, high pressure-rated channels should be used. The proposed fabrication technique summarized in Fig. 1, can be used to extend this separation method [31–33] to higher pressures, since as shown earlier in Fig. 7, the variation of the gap distance is less than 1% for pressures up to 60 kPa and less than 5% for pressures up to 130 kPa.

5 Concluding remarks

The PDMS microchannel deformation is a very important issue in some of the microfluidic applications where precise knowledge of the flow profile, pressure, and channel geometry is needed especially in low aspect ratio microchannels or in assays that while keeping the throughput want to

maintain a small footprint. This paper introduced a novel fabrication technique by utilizing UV curable thiolene resin (such as NOA) coating layer over the stiff PDMS microchannel, which decreases the PDMS deformation more than 70%. The variation of side distance between pillars in the MIMP was studied under high-pressure operation in two different arrays of samples: conventional fabricated samples and glass–stiff PDMS–NOA samples. For the NOA-coated samples, the variation of the gap distance between posts is less than 1% for pressures up to 60 kPa and less than 5% for pressures up to 130 kPa. Finally, the pressure drop in the fabricated samples was determined experimentally and numerically. The obtained results from both separate experiments showed that although the pressure-induced deformation was not completely eliminated by the presented technique, in both cases the deformation was reduced more than 70% in the NOA-coated samples compared to the standard fabrication procedure.

The authors have declared no conflict of interest.

6 References

[1] Samuel, K. S., Whitesides, G. M., *Electrophoresis* 2003, *24*, 3563–3576.

[2] Ciftlik, A. T., Gijs, M. A. M., *Lab. Chip.* 2012, *12*, 396–400.

[3] Gervais, T., El-Ali, J., Günther, A., Jensen, K. F., *Lab. Chip.* 2006, *6*, 500–507.

[4] Zhou, J., Ellis, A. V., Voelcker, N. H., *Electrophoresis* 2010, *31*, 2–16.

[5] Madadi, H., Casals-Terré, J., *Microsyst. Technol.* 2013, *19*, 143–150.

[6] Hardy, B. S., Uechi, K., Zhen, J., Kavehpour, H. P., *Lab. Chip.* 2009, *9*, 935–938.

[7] Khan Malek, C. G., *Anal. Bioanal. Chem.* 2006, *385*, 1351–1361.

[8] Suriano, R., Kuznetsov, A., Eaton, S. M., Kiyan, R., Cerullo, G., Osellame, R., Chichkov, B. N., Levi, M., Turri, S., *Appl. Surf. Sci.* 2011, *257*, 6243–6250.

[9] Huang, Y., Liu, S., Yang, W., Yu, C., *Appl. Surf. Sci.* 2010, *256*, 1675–1678.

[10] Becker, H., Gärtner, C., *Anal. Bioanal. Chem.* 2008, *390*, 89–111.

[11] Tsao, C., DeVoe, D., *Microfluid. Nanofluid.* 2009, *6*, 1–16.

[12] Roy, E., Geissler, M., Galas, J. C., Veres, T., *Microfluid. Nanofluid.* 2011, *11*, 235–244.

[13] Fiorini, G. S., Yim, M., Jeffries, G. D. M., Schiro, P. G., Mutch, S. A., Lorenz, R. M., Chiu, D. T., *Lab. Chip.* 2007, *7*, 923–926.

[14] Kuo, J. S., Chiu, D. T., *Lab. Chip.* 2011, *11*, 2656–2665.

[15] Wägli, Ph., Guélat, B. Y., Homsy, A., Rooij, N. F., *14th International Conference on Miniaturized Systems for Chemistry and Life Sciences*, Groningen, Netherlands, 3–7 October 2010.

[16] Sollier, E., Murray, C., Maoddi, P., Di Carlo, D., *Lab. Chip.* 2011, *11*, 3752–3765.

[17] Hosokawa, K., Hanada, K., Maeda, R., *J. Micromech. Microeng.* 2002, *12*, 1.

[18] Holden, M. A., Kumar, S., Beskok, A., Cremer, P. S., *J. Micromech. Microeng.* 2003, *13*, 412–418.

[19] Inglis, D. W., *Biomicrofluidics* 2010, *4*, 026504.

[20] Odom, T. W., Love, J. C., Wolfe, D. B., Paul, K. E., Whitesides, G. M., *Langmuir* 2002, *18*, 5314–5320.

[21] Choi, K. M., Rogers, J. A., *J. Am. Chem. Soc.* 2003, *125*, 4060–4061.

[22] Armani, D., Liu, C., Aluru, N., *12th International Conference on MEMS 1999*, Orland, FL, USA, pp. 222–227.

[23] Bhattacharya, S., Datta, A, Berg, J. M., Gangopadhyay, S., *J. Microelectromech. S.* 2005, *14*, 590–597.

[24] Kaviany, M., *Principles of Heat Transfer in Porous Media*, Second edition., Springer-Verlag, New York, 1995.

[25] Akbari, M., Sinton, D., Bahrami, M., *J. Fluid. Eng-T, ASME* 2009, *131*, 0412021–0412028.

[26] Murthy, S. K., Sin, A., Tompkins, R. G., Toner, M., *Langmuir* 2004, *20*, 11649–11655.

[27] Lu, H., Koo, L. Y., Wang, W. M., Lauffenburger, D. A., Griffith, L. G., Jensen, K. F., *Anal. Chem.* 2004, *76*, 5257–5264.

[28] Kantak, A. S., Gale, B. K., Lvov, Y., Jones, S. A., *Biomed. Microdev.* 2003, *5*, 207–215.

[29] Gervais, T., Jensen, K. F., *Chem. Eng. Sci.* 2006, *61*, 1102–1121.

[30] Wofsy, C., Goldstein, B., *Biophys. J.* 2002, *82*, 1743–1755.

[31] Di Carlo, D., Irimia, D., Tompkins, R. G., Toner, M., *PNAS* 2007, *104*, 18892–18897.

[32] Di Carlo, D., *Lab. Chip.* 2009, *9*, 3038–3046.

[33] Davis, J. A., Inglis, D. W., Morton, k. J., Lawrence, D. A., Huang, l. R., Chou, S. Y., Sturm, J. C., Austin, R. H., *PNAS* 2006, *103*, 14779–14784.

